# 4. Injection System

The injection system of the synchrotron light source CANDLE is composed of a 100 MeV electron injector linac followed by 3 GeV full energy booster synchrotron. A 3 GHz electron linac accelerates the electrons up to an energy of 100 MeV that are injected into the booster synchrotron with the frequency of the RF system of 500MHz. Each three bunches from the linac fill one RF bucket of the booster synchrotron. After ramping, the energy of the electrons in the booster increases from injection energy of 100 MeV to final energy of 3 GeV in 0.5 sec (repetition rate 2 Hz), at which time the beam is injected into the main storage ring. Due to longitudinal damping of the energy oscillation in the booster, an extracted electron beam has a time structure that exactly fits with the RF frequency of 500 MHz for of the storage ring. The nominal beam current of the booster of 5 mA enables the storage of the required 350 mA circulating current in the main ring in less than 1 min. The injection system enables single and multi-bunch operation modes of the main storage ring with a flexible variation of the beam time structure according to synchrotron radiation users demand.

## 4.1 Booster Synchrotron. Magnetic system.

The original booster design [1] for the CANDLE light source was based on the following conservative considerations:

- To have independent easy access to booster synchrotron during storage ring operation;
- A small booster geometry (about ½ storage ring circumference) located in inner space of the storage ring.

Although such considerations for the design of the booster synchrotron meets with the necessary requirements of the facility operation, some disadvantages of such an approach are well known from an economic and layout points of view, namely:

- Ineffective use of the available inner space of the storage ring;
- Additional necessary separate shielding walls for the booster;
- High cost of the associated machine building;
- Comparatively high field of the booster bending magnets and the high power supply requirements;
- Comparatively higher energy loss in the form of synchrotron radiation and higher power requirements for the RF system;
- Comparatively large horizontal beam emittance at extraction energy of 3 GeV (400nm).

The detail analysis of these features, the experience gained with the SLS facility [2] and the analysis performed for the DIAMOND project [3] lead to the revision of the basic approaches to the booster synchrotron design for the CANDLE source. The booster is designed to fit at the same tunnel where the main storage ring will be located, at the inner diameter of the storage ring tunnel. The booster has a four fold symmetry super-lattice structure with a circumference of 192 m that compares to storage ring circumference in the ratio of 8/9. To avoid effects of stray fields upon the storage ring, an average distance between two rings is 3.8 m.

The choice of the option of larger diameter booster close in size to the main ring diameter for CANDLE has been based on a comparative analysis of the booster performance for the medium size (200-300 m in circumference) facilities like SLS (288m), CANDLE (216m) and larger size facilities (300-400m in circumference) like DIAMOND (397m) and SOLEIL (354m). For the medium storage ring circumferences, increasing the nominal booster ring leads to reasonable machine improvement and cost saving, while for the larger facilities a larger diameter booster results in higher civil engineering costs which in turn reverse any saving from the accelerator complex. The general layout of the accelerator complex with the modified booster ring is shown in Fig. 4.1.1. The reference orbits of two rings are positioned at the same level as shown.
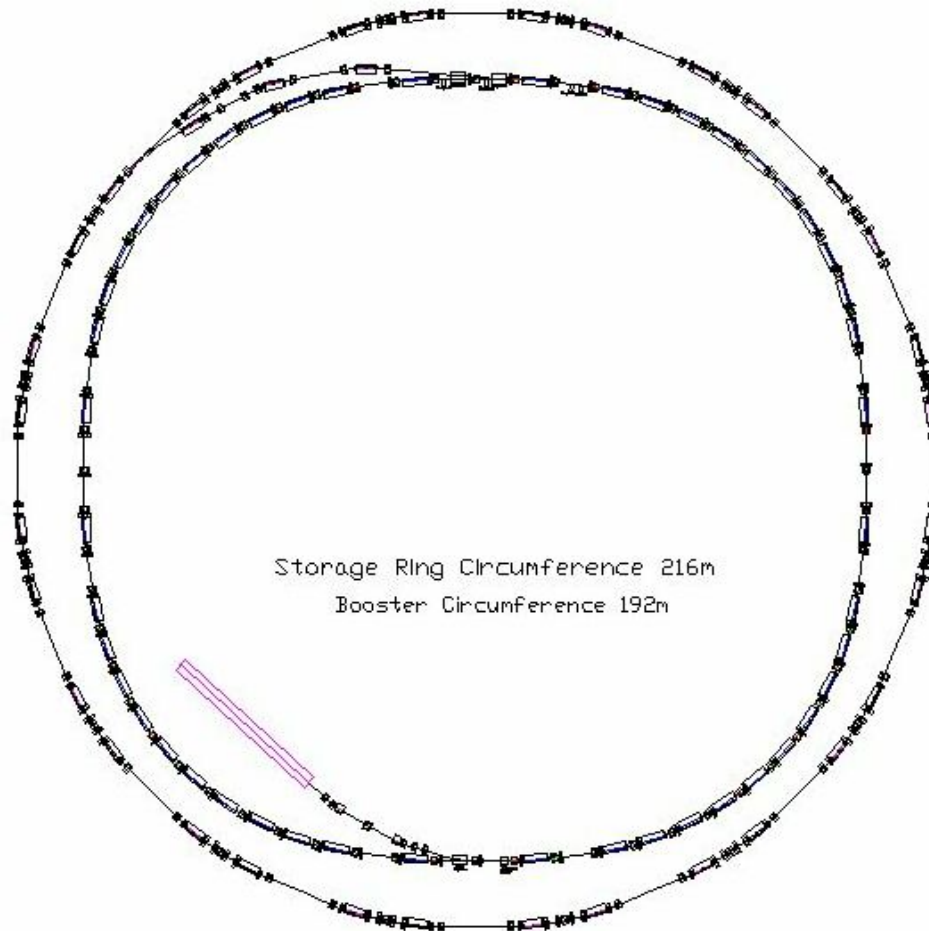


Storage Ring Circumference 216m
Booster Circumference 192m

**Fig. 4.1.1 Schematic layout of CANDLE accelerator complex.**

The main advantages of the modified large booster are:

- saving in building space and reduced shielding costs
- economic magnets with small aperture
- reduced total RF power
- flexible repetition rates and ramping profiles
- efficient and fast injection into the storage ring
- simplified vacuum chamber
- small beam emittance

The absence of the separate access to the booster ring is compensated with an effective diagnostic and control system at any stage of the machine operation.

137

## 4.1.1 Booster Lattice

The main considerations that underline the booster lattice design are:

- A full 3 GeV energy synchrotron;
- Minimum filling time with possible maximum current;
- High level flexibility for lattice functions and working point;
- Low beam emittance for effective injection into the storage ring;
- Long dispersion free straight sections for injection/extraction and RF accommodation;
- Low dipole fields and repetition rate.
- Minimum beam losses during injection, acceleration and extraction.

After the detailed analysis of various types of magnetic systems, a four fold symmetry FODO structure lattice with missing dipoles was selected to meet the above requirements in machine design. Fig. 4.1.2 shows the magnetic structure per one quadrant of the booster. A quadrant of the booster lattice consists of 16 cells, 4 of which are without dipoles. The entire lattice contains 48 separated function dipole magnets, each with a bending angle $7.5^0$. The bending magnetic field is 0.727 T at the maximum energy 3 GeV, corresponding to a bending radius of 13.751 m. The booster circumference of 192 m ( 8/9 of the storage ring circumference) provides the harmonic number 320 for the RF frequency of 500 MHz. Because RF cavities and the injection and extraction devices are installed into the empty cells, dispersion must be eliminated in these sections. The number of FODO cells and the betatron phase advance per cell have been chosen to cancel the dispersion function in the straight section with only two sets of quadrupoles .

The magnetic lattice has a good injection efficiency with a large dynamic aperture for the machine at an injection energy 100 MeV from the linac and provides for a small horizontal beam emittance of 75 nm-rad at full extraction energy. The 5 mA nominal pulse current with a repetition rate of 2 Hz enables filling the 350 mA stored current in the main ring in less then two minutes for the different operational modes.

The beam optics simulations for the booster were done using code OPA [4] and the closed orbit distortions and correction were calculated by program MAD [5].

The amplitude functions for the one quadrant of the ring are shown in Fig. 4.1.3.



**Fig.4.1.2 Schematic layout of the one quadrant of booster lattice.**

.

Betafunctions [m]                                          $\eta_X$ [m]

* 10

| | |
|---|---|

4*L = 192.00 m        Qx =   9.1876   Qz =   6.2407   Ex = 7.50E-0008
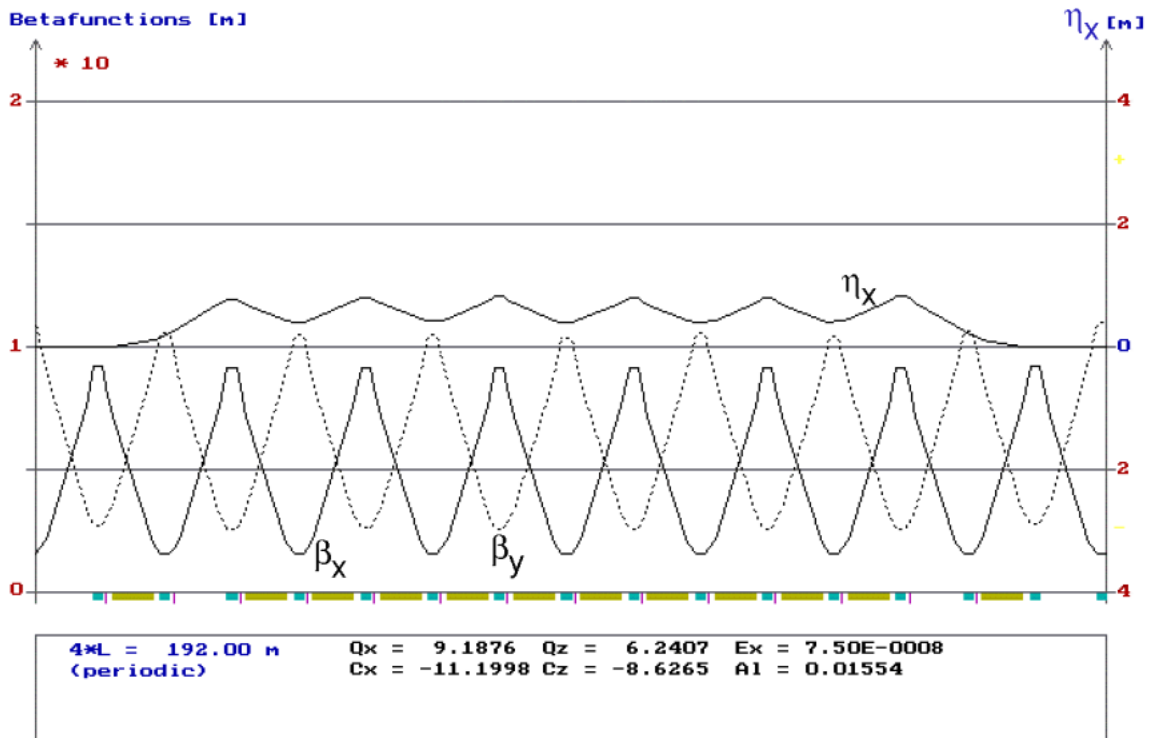(periodic)            Cx = -11.1998 Cz = -8.6265   Al = 0.01554

**Fig.4.1.3 Booster optic functions per one quadrant.**

The tune values for the betatron oscillations in the horizontal and vertical plane have been optimized to obtain a low horizontal emittance for the beam of 75 nm-rad with moderate strength quadrupole magnets fields. In addition, the maximum betatron functions in the horizontal and vertical planes are kept at the level of 10 m (8.5 m for horizontal beta, 12.2 m for vertical beta) to reduce the distortions of the central trajectory in a misaligned machine, thus improving the stability of machine operation. The working point of the betatron oscillations in the resonance diagram (Fig. 4.1.4) corresponds to betatron tunes $Q_x = 9.187$ (horizontal) and $Q_y = 6.24$ (vertical). Simulation results of the ramping process indicate a working point which does not cross any strong resonance lines (low order resonance lines in tune diagram).
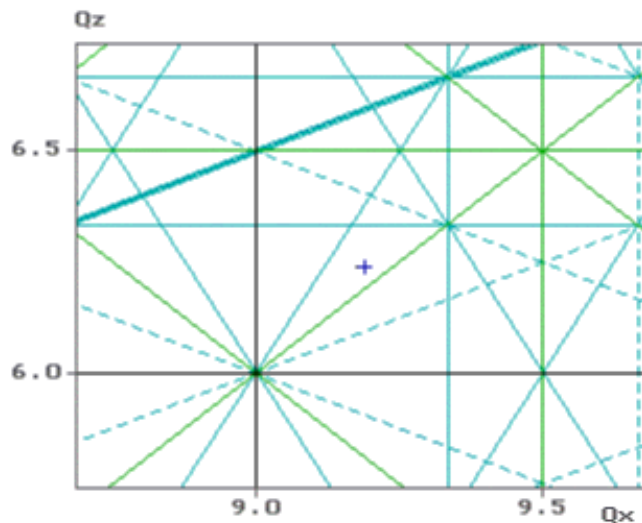


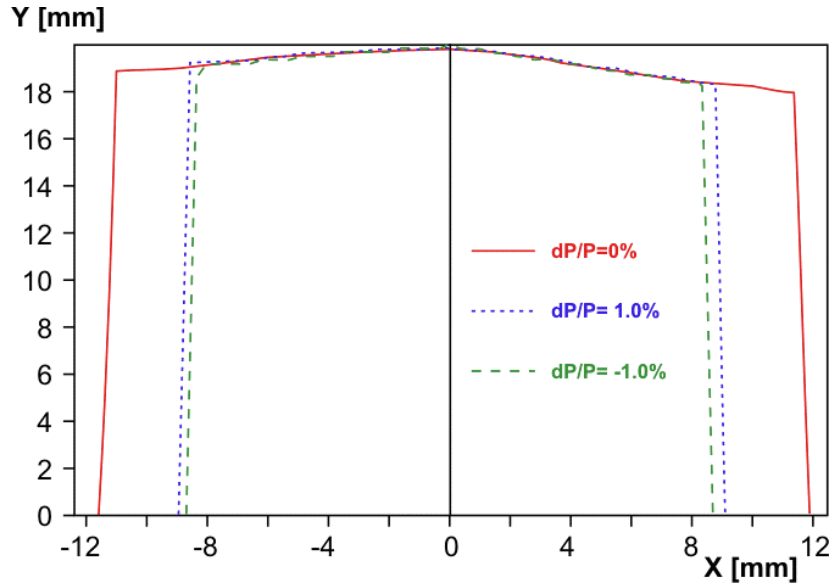**Fig 4.1.4 Booster working point for tunes and resonance diagram.**

139

**Fig.4.1.5 Booster dynamic aperture (no errors). For off momentum particles with $\Delta p/p = \pm 1\%$ the dynamic aperture is $|x| = 9mm$ in the horizontal plane at the injection point.**

Two sets of sextupoles (14 focusing and 14 defocusing) compensate for the natural chromaticity of the machine: $\xi_x = -11.2$ in horizontal and $\xi_y = -8.62$ in vertical planes, respectively. The focusing and defocusing sextupole magnets are located near the focusing and defocusing quadrupole magnets of the normal FODO cell. The calculated values of focusing and defocusing sextupole strength for the chromaticity compensation are 10.3 m$^{-3}$ and 17.2 m$^{-3}$ respectively.

The resulting dynamic aperture (see Fig 4.1.5) of the lattice is larger than the physical aperture and for the $\pm 1\%$ off-energy particles provide for 9mm stable oscillations at the injection point. The nonlinear tune shift dependent energy chromaticity study for the booster (Fig. 4.1.6) shows very flexible operation of the machine with the given magnetic structure and a tune shift that minimizes the beam losses during injection, acceleration and extraction processes. The beam envelope along the booster lattice at the extraction energy of 3 GeV (Fig. 4.1.7) also indicates excellent performance of the electron beam in a modified booster option with the larger circumference.
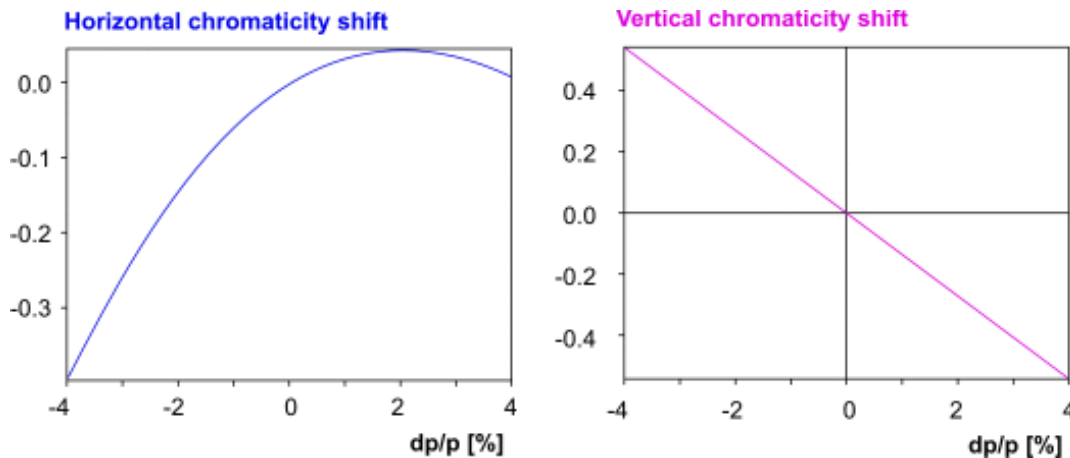


**Fig.4.1.6 Horizontal (left) and vertical (right) chromaticity dependence of momentum spread.**
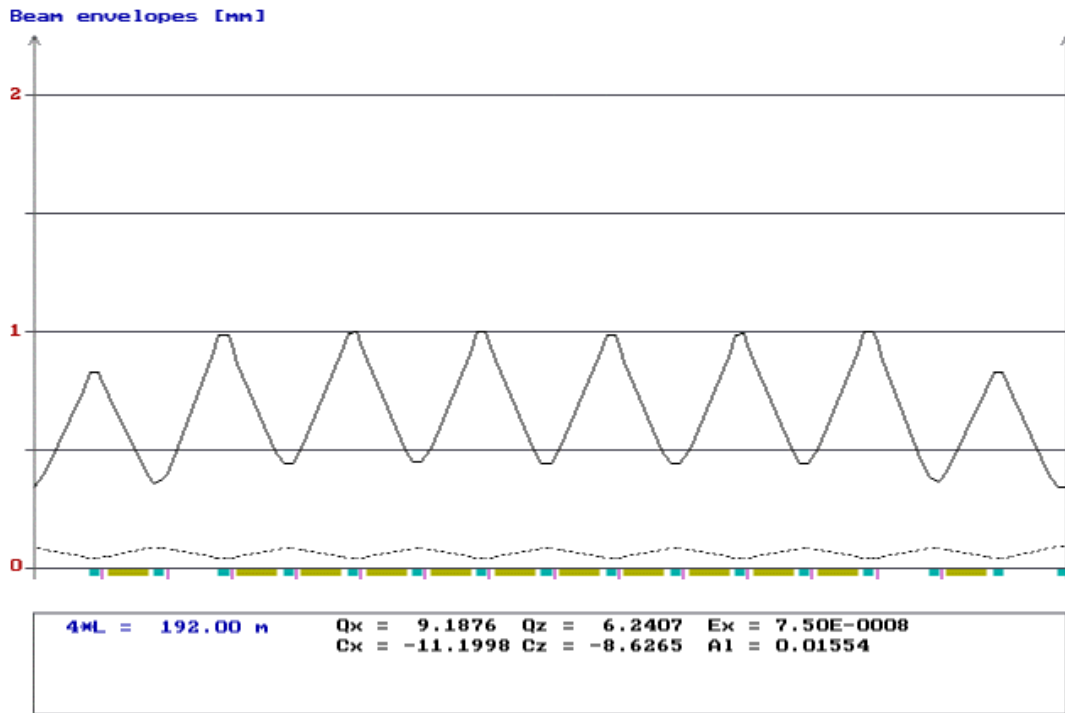
140

**Fig.4.1.7 Beam horizontal and vertical envelopes at extraction energy 3 GeV.**

The main parameters of the booster synchrotron are given in Table 4.1.1. Note, that the booster magnetic structure provides a damping of oscillations for all three degrees of freedom: horizontal, vertical and longitudinal. The features of low repetition rate and controllable energy ramp for the booster make the machine very flexible in controlling the time structure of the injected beam into the storage ring and dynamical control of the filling process.

**Table 4.1.1 Booster main parameters.**

| | |
|---|---|
| Circumference (m) | 192 |
| Injection energy (MeV) | 100 |
| Extraction energy (GeV) | 3 |
| Straight section length (m) | 2.6 |
| Cycling rate (Hz) | 2 |
| Lattice type | FODO |
| Hor. emittance (nm.rad) | 74.9 |
| Energy spread | $6.9 \ 10^{-4}$ |
| Energy loss/turn (keV) | 521.04 |
| Max.($\beta_x, \beta_y, \eta_x$)(m) | 8.5; 12.2; 0.48 |
| Number of periods | 4 |
| Bending magnet field (T) | 0.7272 |
| Bending radius (m) | 13.751 |
| Harmonic number | 320 |
| RF frequency (MHz) | 499.564 |
| Tunes (horizontal/vertical) | 9.19/6.24 |
| Natural chromaticities | -11.19/-8.63 |
| Damp. Times ($\tau_x, \tau_y, \tau_s$)(ms) | 7.6; 7.4; 3.6 |
| Momentum comp. factor | 0.0155 |

141

## 4.1.2 Misalignments and Closed Orbit Correction

For providing for beam position diagnostics, 24 (6 in each superperiod) beam position monitors are installed in the booster lattice. For closed orbit corrections 48 magnetic correctors (24 for horizontal plane and 24 for vertical plane) are chosen. The level of precision for the closed orbit compared to the ideal design orbit was taken to be about 0.2 mm. The main sources for closed orbit distortions (COD) are assumed to be the integrated field errors in the dipoles, alignment errors of the dipole and quadrupole magnets and rotational errors around the vertical, horizontal and longitudinal axis. The tolerances for these errors are given in the Table 4.1.2 for the dipole magnets and in Table 4.1.3 for the quadrupole magnets, respectively.

**Table 4.1.2 Installation tolerances for dipole magnets**

| | | |
|---|---|---|
| Integral field $\Delta(B \cdot l)/(B \cdot l)_0$ | | $10^{-3}$ |
| Horizontal position , | $\Delta_x$ (m) | $10^{-3}$ |
| Vertical position, | $\Delta_y$ (m) | $5\ 10^{-4}$ |
| Longitudinal position, | $\Delta_s$ (m) | $10^{-3}$ |
| Rotation around hor. axis , | $\Delta_{\theta x}$ (rad) | $10^{-3}$ |
| Rotation around vert. axis , | $\Delta_{\theta y}$ (rad) | $10^{-3}$ |
| Rotation around long. axis , | $\Delta_{\theta s}$ (rad) | $5\ 10^{-4}$ |

**Table 4.1.3 Installation tolerances for quadrupole magnets.**

| | | |
|---|---|---|
| Horizontal position , | $\Delta_x$ (m) | $2\ 10^{-4}$ |
| Vertical position, | $\Delta_y$ (m) | $2\ 10^{-4}$ |
| Rotation around hor. axis, | $\Delta_{\theta x}$ (rad) | $10^{-3}$ |
| Rotation around vert. axis , | $\Delta_{\theta y}$ (rad) | $10^{-3}$ |
| Rotation around longit.. axis , | $\Delta_{\theta s}$ (rad) | $5\ 10^{-4}$ |

The beam closed orbit distortions generated by random errors in the dipole and quadrupole magnets is shown in Fig. 4.1.8. The closed orbit distortion is at a level of 2-3mm in both the horizontal and vertical plane of oscillations. The first iteration in the correction procedure based on identical kicks by corrector magnets results in a reduction of factor of 3 in the disturbed orbit and stabilizes the disturbed orbit to a levels of 0.5 mm in horizontal and 1 mm in vertical planes, respectively (Fig. 4.1.9). The fine correction of the disturbed orbit based on BPM measurements and individual correction scheme provides a stabilization to a level of 0.3 mm in both planes.
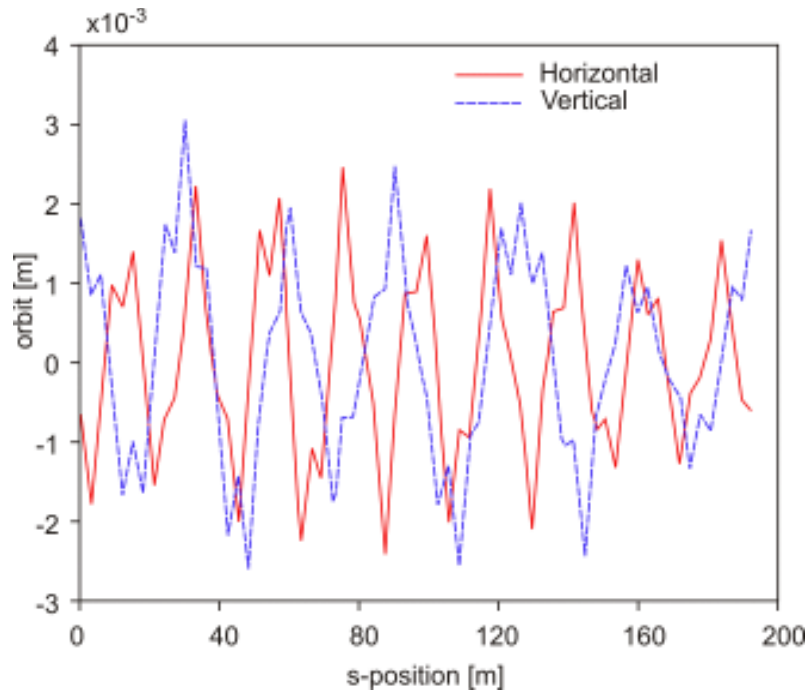
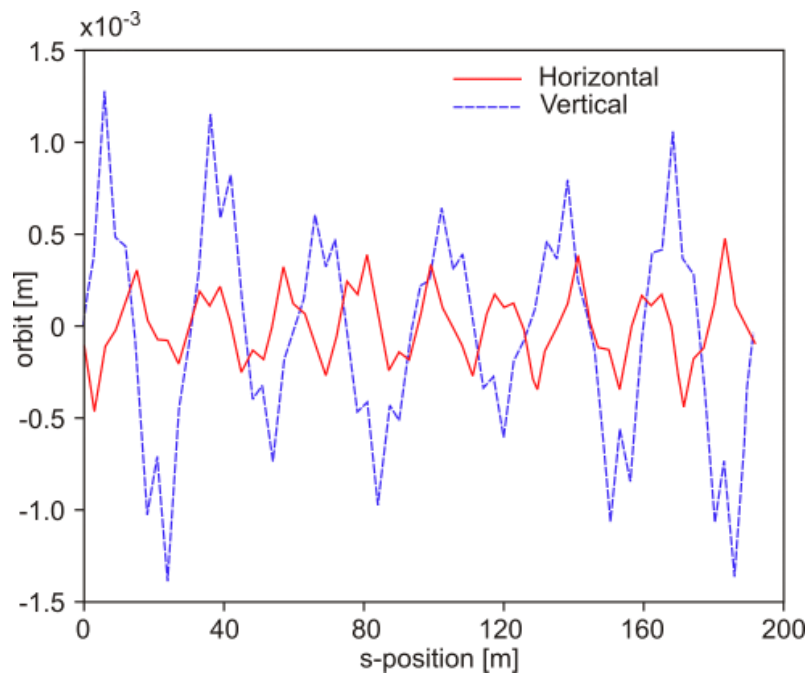**Fig. 4.1.8 Beam closed orbit distortion (before correction).**



**Fig. 4.1.9 Beam closed orbit distortion (after correction).**

## 4.1.3 Injection and Extraction

The 3 GeV booster synchrotron has a four fold symmetry super-lattice structure with straight sections of 3.5 m length. Two of these straight sections will be used for the injection of the 100 MeV electron beam from the linac and extraction of the 3 GeV beam from the booster. Injection will be performed in one turn with the beam pulse from the linac filling 240 RF buckets of the booster from the 320 buckets available. The 80 free buckets provides a time interval of 160 ns for the fields of the injection and ejection

143

kickers to decay. Ejection of the beam from the booster will be performed based on a slow bump (3 kickers) with a further fast kick (1 kicker) of the beam. The ejection time will be tunable as an integer number of 500 MHz pulse length of 2 ns to fill an appropriate part of the storage ring. The energy ramping process in the booster will be controllable so that the full energy beam can be kept in the booster the necessary time before the beam ejection to storage ring. This will not affect the beam quality as the booster has a separate function magnetic system with radiation damping in all three degree of freedom.

**Injection.** Beam will be injected into the booster central orbit using a single-turn injection scheme with the help of a septum magnet and a fast kicker magnet. The design aims to achieve the transfer with minimum beam loss and beam emittance dilution. The optical parameters of the injection channel $\alpha, \beta$ in horizontal and vertical planes are exactly matched with corresponding Twiss parameters at the exit of the injection septum. The injection straight section of the booster is dispersion free so that dispersion in the horizontal plane becomes zero after the geometrical matching with the central trajectory.

The injection scheme is shown schematically in Fig 4.1.10. The 100 MeV electron beam after the final focusing quadrupole QF of linac-booster transfer line enters the 0.6 m septum magnet with the magnetic filed of 0.144 T which bends the incoming electron beam by about 14 degree. The thickness of the septum is 3mm and it is located at a distance of 22 mm from the reference orbit of the ring.
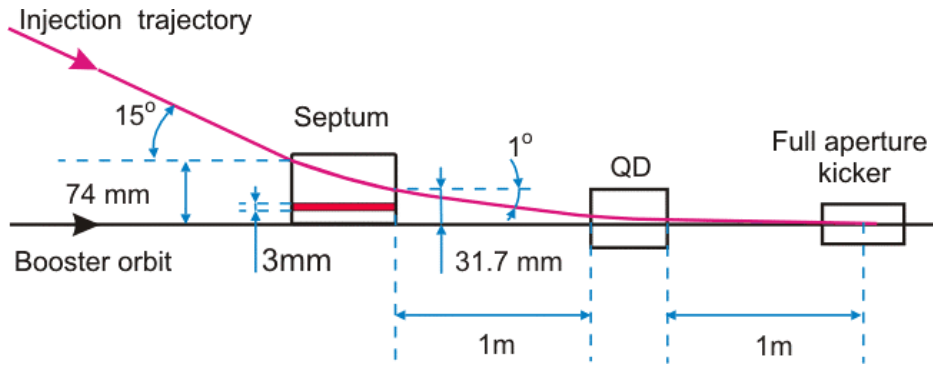


**Fig 4.1.10 Schematic layout of booster injection**

For horizontal injection, the center of the injected beam was calculated to be at a distance $x$ from the ideal design orbit at the exit of the septum:

$$x = n_1 \cdot \sqrt{\beta_i \cdot \varepsilon_i} + n_2 \cdot \sqrt{\varepsilon_x \cdot \beta_x} + \eta_x \cdot ((\Delta p / p)_i + (\Delta p / p)_x) + x_c + x_s \qquad (4.1.1)$$

where $\varepsilon_i$ is the horizontal emittance of injected beam, $(\Delta p / p)_i$ is the corresponding momentum spreads, $x_c$ is an allowance for closed orbit deviation and clearances, $x_s$ is the effective thickness of the septum, $\eta_x$ is the horizontal dispersion at the septum exit, $n_1$ and $n_2$ are the numbers of sigmas for the injected and stored beams, respectively

The septum magnet is located in one of the straight sections of the booster ring with the exit located at 0.3m behind the middle of the straight section. The entrance to the fast kicker magnet is located at a position of 2.15m downstream from the septum exit. The injection section is dispersion free and is matched with the injection channel so that $\eta = 0$.

With $\beta_x = 6.4m$, $\varepsilon_i \approx 10^{-6} m \cdot rad$, $(\Delta p / p)_i = 2 \cdot 10^{-4}$, $\eta_x = 0$, $x_c = 3mm$ and $x_s = 3mm$ from the (1) we obtain (including some 3mm overestimation for steering errors) the injected beam position at the septum exit $x = 31.7mm$.

Injected beam delivered by linac is directed to the injection septum at the angle of $15^0$ in respect to the booster straight section axis at the distance of 74mm from the axis. The septum deflects the beam by the angle of $14^0$ and forwards it to the defocusing quadrupole magnet at the angle $1^0$. The beam enters the QD magnet at the horizontal distance of 15.7 mm from the axis and exits at the distance of 10.5 mm getting the kick of 5.4mrad. The deflection angle that the kicker must then impart to the beam to move it subsequently on the design orbit is 10.6 mrad.

The relative position of the injected beam to the septum and the reference orbit of the booster are shown in Fig. 4.1.11.
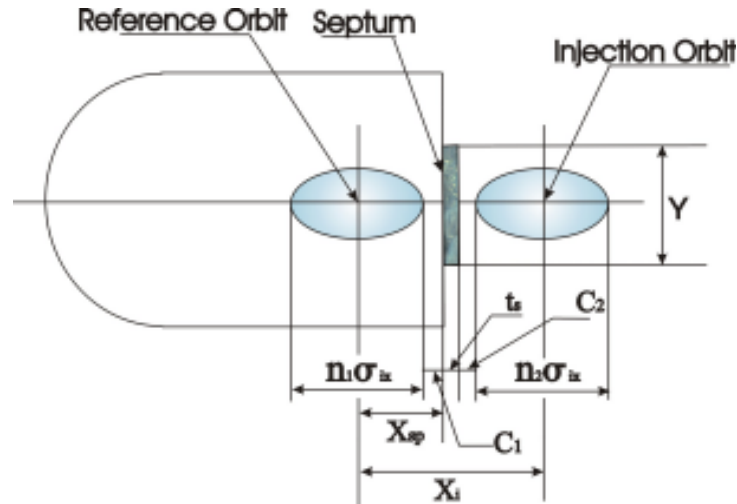


**Fig. 4.1.11 Beam positions at the injection**

The parameter list of the injection point is given in Table 4.1.4

**Table 4.1.4 Optic parameters at injection**

| Beam size | $\sigma_{ix}$=4.5mm |
|---|---|
| Number of sigmas | $N_1$=4 |
| Number of sigmas | $N_2$=4 |
| Clearance | $C_1$=3.0mm |
| Clearance | $C_2$=1.2mm |
| Septum Thickness | $t_s$=3mm |
| Septum Position | $X_{sp}$=22mm |
| Injection Orbit | $X_i$ =74mm |
| Beta function at injection | 6.4m |

The kicker magnetic field is given by

$$B_k = (B \cdot \rho) \cdot \theta / L ,\qquad (4.1.3)$$

where $B \cdot \rho = 1/3Tm$ is the electron magnetic rigidity at 100 MeV injection energy, $L = 0.5m$ is the kicker length. The required 10.6mrad kick for beam is provided by the magnetic field of $B = 7.1mT$. The kicker maintains a steady field during the 480 ns passage time for the injected beam (240 RF buckets of 500 MHz frequency) and then decays with a lifetime of 160 ns, substantially shorter than the time for the injected bunch to return to the kicker magnet after one turn.

The maximum width and height of the injected beam in the $3\sigma$ contour are $5.4mm$ and $4.2mm$ respectively. Taking into account alignment errors and leaving some space for beam steering, the septum aperture is taken to be $45mm \times 20mm$. The kicker aperture is mostly determined by orbit deviations and pumping speed considerations and is specified to be $40mm \times 25mm$. The design specifications of the septum and kicker magnets are given in the section on booster sub-systems.

**Extraction**. Many features of extraction are the reverse process of injection, however, the extraction process has a specific requirements coupled with the high beam energy, namely the necessity for creation of a closed slow bump followed by a fast kick for the accelerated beam. The extraction channel begins at the long straight section opposite to the injection section. The relatively high energy of the extracted beam requires two subsequent septum magnets with thin and thick septa.

The arrangement of the three bumper magnets, the two septum magnets and the fast kicker magnet at booster extraction region with the bumped orbit created by three bumper magnets is shown in the Fig. 4.1.12.

After a local closed orbit bump of 14.9 mm created by three slow kickers K1, K2 and K3 (bumper magnets), the circulating beam is extracted in one turn using a fast kicker and two pulsed septum magnets. The extraction fast kicker K4 magnet deflects the beam 0.67 mrad into the aperture of a thin (passive) septum magnet, which in turn bends the beam at $3^o$ into a thick (active) septum that produces the final extraction trajectory from the booster at $8^o$ into the booster-to-storage ring transfer line (BTR). This angle is sufficiently large to avoid beam hitting the booster magnets.
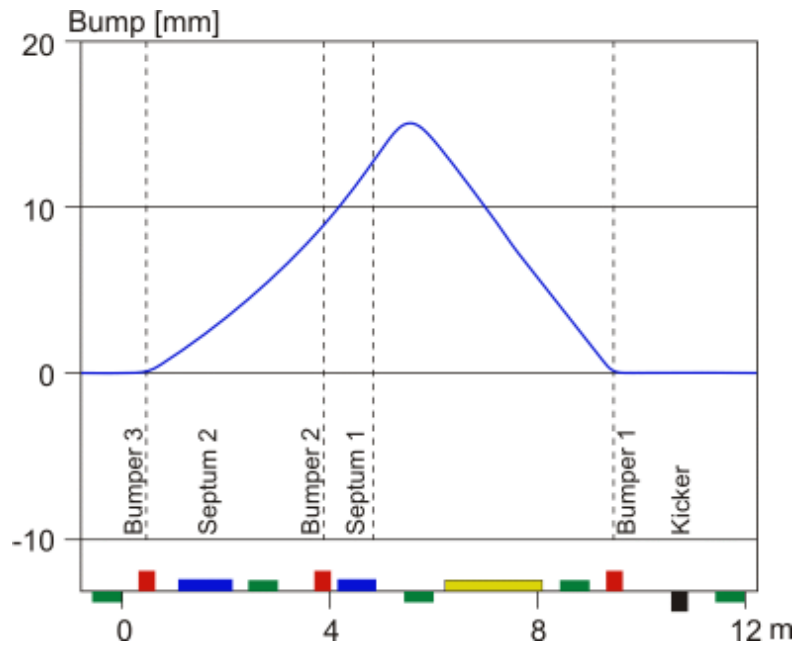


**Fig 4.1.12 Bumped orbit at booster extraction.**

The 0.8 m long thin septum magnet has a nominal magnetic field of 0.44 T. The septa thickness is 2mm. The thick septum magnet has a length of 1.1 m and a magnetic field of 0.64 T. Note that the given arrangement of the extraction system for the booster permits multi-turn ejection of the beam based on the beam "shaving" mechanism. This option can be applied for the top-up injection into the storage ring when very low currents (~0.1mA) are required to restore the stored beam current in the main ring to its nominal level of 350 mA. Table 4.1.5 presents the main parameters of the booster extraction channel.

**Table 4.1.5 Parameters of extraction system.**

| | |
|---|---|
| Bump offset at the septum entrance (mm) | 14.9 |
| Septum location with respect to orbit (mm) | 18 |
| Aperture of thin septum | $15mm \times 6mm$ |
| Aperture of thick septum | $15mm \times 6mm$ |
| Field in thin septum (T) | 0.44 |
| Field in thick septum (T) | 0.64 |

## 4.1.4 Magnet Parameters

**Regular lattice.** The magnetic lattice of the booster synchrotron consists of 48 separate function dipole magnets, 64 quadrupole magnets, 28 sextupole magnets and 32 steering magnets. The main parameters of the booster magnets are listed in  Table 4.1.6.

**Table 4.1.6  Booster lattice magnets parameters**

| Magnet type | Nominal Value | Max. Limit |
|---|---|---|
| **Dipoles** | | |
| Quantity | 48 | |
| Gap height  (mm) | 30 | |
| Effective length (m) | 1.80 | |
| Dipole Field (T) | 0.723 | 1.4 |
| **Quadrupoles** | | |
| Quantity | 64 | |
| Aperture radius (mm) | 20 | |
| Effective length  (m) | 0.4 | |
| Gradient QF/QD (T/m) | 13.3/-10.07 | 18 |
| **Sextupoles** | | |
| Quantity | 28 SF; 28 SD | |
| Aperture radius (mm) | 20 | |
| Effective length (m) | 0.15 | |
| Strength  SF/SD $(T/m^2)$ | 90.7 /-114.6 | 200 |

**Injection system.** The injection system consists of one septum magnet and one fast kicker magnet. The magnets parameters are given in Table 4.1.7.

**Table 4.1.7 Parameters of booster injection magnets.**

| Septum | |
|---|---|
| Magnetic length | 0.6 m |
| Nominal deflection | 258.3 mrad |
| Magnet field | 0.144 T |
| Circulating beam aperture | unrestricted |
| Aperture | 20mmx15mm |
| Magnet current waveform | half-sine, 70 $\mu s$ |
| **Fast Kicker** | |
| Magnetic length | 0.5 |
| Nominal deflection | 3.5 mrad |
| Magnet field | $2.3 \ 10^{-3}$ T |
| Aperture | 40mm x 25mm |
| Magnet current waveform | 150 / 480 / 150ns |

**Extraction system.** The extraction system consists of three slow kicker magnets, one fast kicker magnet, thin and thick septum magnets whose parameters are listed in Table 4.1.8.

**Table4.1.8. Main parameters of booster ejection thin septum.**

| Thin Septum | |
|---|---|
| Magnetic length | 0.8 m |
| Nominal deflection at 3 GeV | 34.9 mrad |
| Magnetic field | 0.436 T |
| Septum thickness | 2 mm |
| Extracted beam aperture | 15mmx6mm |
| Magnet current waveform | Half-sine,70 $\mu s$ |
| **Thick Septum** | |
| Magnetic length | 1.1 m |
| Nominal deflection at 3 GeV | 69.8 mrad |
| Magnetic field | 0.635 T |
| Septum thickness | 3 mm |
| Extracted beam aperture | 15mmx6mm |
| Magnet current waveform | Half-sine,70 $\mu s$ |
| **Slow kickers ( bumpers)** | |
| Number of bumpers | 3 |
| Magnetic length | 0.5 m |
| Nominal deflection at 3 GeV | 2.4/1.0/3.4 mrad |
| Magnet field | 48/20/78 mT |
| Magnet aperture | 60mmx26mm |
| **Fast Kicker** | |
| Magnetic length | 0.5 m |
| Nominal deflection at 3 GeV | 0.67 mrad |
| Magnet field | 13.4 mT |
| Magnet aperture | 60mmx20mm |
| Magnet current rise time | 150 ns |
| Magnet current top | 200 ns |

## References

1. Martirosyan Y.  Tsakanov V. and Grigoryan B., " Booster Synchrotron for CANDLE Light Source", Proc. SSILS, Shanghai, China, 2001.
2. SLS Handbook, PSI, Villigen, 1999.
3. Marks N. et al.,  " The Economic Optimisation of the Main Parameters of the 3 GeV Electron Booster Synchrotron for the DIAMOND", Proc. EPAC'00,Vienna.
4. Streun A. OPA code documentation, PSI, Villigen, 1997.
5. Owen H., MAD Version 8.23DL, DPG-XX-rpt-006, 2000,